Small-Angle X-ray Scattering from Poly(vinyl acetate) Solutions and Networks Swollen in Acetone

Anne-Marie Hecht, Ferenc Horkay,† and Erik Geissler*

Laboratoire de Spectrométrie Physique,‡ Université J. Fourier de Grenoble, B.P. 87, 38402 St. Martin d'Hères Cedex, France

Jean Pierre Benoit

Laboratoire pour l'Utilisation du Rayonnement Electromagnétique, Centre Universitaire Paris-Sud, 91405 Orsay Cedex, France

Received December 4, 1990; Revised Manuscript Received February 28, 1991

ABSTRACT: Small-angle X-ray scattering (SAXS) measurements are reported for semidilute poly(vinyl acetate) (PVAc) solutions and gels in good solvent conditions. The results for the solutions are in agreement with the predictions of scaling theory and consistent with the osmotic properties of these solutions obtained from the literature. The correlation length ξ follows a power law behavior in polymer volume fraction φ, where

$$\xi = (2.2 \pm 0.2)\varphi^{-0.75\pm0.03}\ \text{Å}$$

The gel spectra are compared to those of the solutions, and the second moments describing the static concentration fluctuations are evaluated. A solution-like component is distinguished in the gel signal, the intensity of which is close to that calculated from independent osmotic measurements performed on the same samples. The effective concentration of this component proves to be smaller than the mean concentration of the swollen network.

Introduction

In recent years much effort has been devoted to the study of the structure and behavior of swollen network systems. Among the techniques used, small-angle neutron and dynamic light scattering have been prominent.[1-6] Although small-angle X-ray scattering has been used for the study of polymer solutions,[7,8] rather fewer investigations have applied this method to gels. Synchrotron sources have made available high-intensity X-ray beams whose incident wavelength is known with great precision. In combination with multidetectors, this permits measurements of high signal-to-noise ratio to be made in a relatively short time.

In the present investigation our aim is to examine the X-ray scattering properties of a set of polymer solutions at different concentrations in a good solvent and to compare these spectra with those of gels fully swollen in the same diluent. The solution spectra are used to calibrate the intensities of the gel spectra. An attempt is made to derive the macroscopic osmotic and swelling properties from the results and to compare these with the corresponding data determined independently by macroscopic methods.

Theoretical Background

Scattering. For a polymer solution at volume fraction φ, the scattering intensity is governed by the amplitude of the concentration fluctuations, $\langle \Delta\varphi^2 \rangle$, which is inversely proportional to the osmotic compressional modulus K_{os}. The resulting X-ray scattering intensity $I(Q)$ is given by[9]

$$I(Q) = a\frac{kT(\rho_p - \rho_s)^2\varphi^2}{K_{os}}S_S(Q) \qquad (1)$$

where a is a constant that depends on the incident wavelength and on the scattering geometry used, k is the Boltzmann constant, T is the absolute temperature, ρ_p and ρ_s are the electron densities of the polymer and the solvent, respectively, $S_S(Q)$ is the structure factor of the solution, and $Q = (4\pi/\lambda)\sin(\theta/2)$ is the transfer wave vector for an incident wavelength λ and scattering angle θ.

For semidilute solutions at small values of Q the structure factor can be approximated by an Ornstein-Zernicke type equation

$$S_S(Q) = 1/(1 + Q^2\xi^2) \qquad (2)$$

where ξ is the density–density correlation length in the solution.

In a cross-linked system, on account of the finite elastic modulus G, the expression for the intensity scattered by the concentration fluctuations is determined not just by K_{os} but also by the longitudinal osmotic modulus, $M_{os} = K_{os} + 4G/3$.[10] In such systems, however, diffusion of the polymer segments is partially restricted, and regions of excess polymer content build up that appear as permanent departures from uniformity. The mean square amplitude of such static excursions is denoted $\langle \delta\varphi^2 \rangle$, and their existence renders eq 1 incomplete as a description of the gel scattering spectrum. The polymer distribution may be viewed as a static structure, with movements of limited amplitude occurring around some average (or slowly varying) position. Thus the total mean square amplitude of the concentration fluctuations may be approximated by the sum of two parts, a dynamic plus a static part:

$$\langle \Delta\varphi^2 \rangle = \langle \Delta\varphi^2 \rangle_{dyn} + \langle \delta\varphi^2 \rangle \qquad (3)$$

For the structure factors of each of these contributions, it has been previously suggested[11] that the dynamic part be represented by a solution-like response analogous to eq 1 (with M_{os} replacing K_{os}), where the structure factor has the same form as eq 2. The structure factor of the static component depends upon the type and distribution of the nonuniformities and hence on the details of the gelation procedure. Cross-linking of the polymer solution is

† On leave of absence from the Department of Colloid Science, Eötvös Loránd University, Budapest, Hungary.
‡ CNRS associate laboratory.

0024-9297/91/2224-4183$02.50/0

accompanied by rearrangements of the polymer within the volume V of the sample but usually introduces only marginal changes in the overall composition of the system. Consequently, although the shape of the scattering function $I(Q)$ will in general be modified by the changes in configuration, the total second moment

$$M_2 = \frac{1}{4\pi}\int_0^\infty I(Q)\exp(i\mathbf{Q}\cdot\mathbf{r})\,d\mathbf{Q}|_{r=0} = \int_0^\infty I(Q)Q^2\,dQ = 2\pi^2 V(\rho_p - \rho_s)^2\langle\Delta\varphi^2\rangle \quad (4)$$

remains invariant.[12]

According to eq 3, M_2 contains two components, whose separation requires the independent determination of either the static or the dynamic contribution to the spectrum. As a first approximation, we assume that the dynamic part of the spectrum can be identified with that of a solution of the same concentration. This assumption implies that the osmotic properties of the network chains are identical with those of the polymer in solution and also that $\langle\delta\varphi^2\rangle$ is much smaller than $\langle\Delta\varphi^2\rangle$. Knowledge of $\langle\delta\varphi^2\rangle$ obtained via this procedure is of importance in the characterization of gels, since it is one of the rare quantitative criteria that define the nonuniformity of the network structure.

Osmotic Properties. The thermodynamic properties of polymer solutions are defined by the osmotic pressure Π. In the theory of Flory and Huggins,[13] Π is given by the expression

$$\Pi = -(RT/v_1)[\ln(1-\varphi) + (1-P^{-1})\varphi + \chi\varphi^2] \quad (5)$$

where χ is the polymer–solvent interaction parameter, v_1 is the partial molar volume of the solvent, and P is the degree of polymerization. Scaling theories of polymer solutions[9,14,15] predict a power law behavior for the concentration dependence of the osmotic pressure in the asymptotic semidilute regime (i.e., $P \to \infty$, $\varphi \ll 1$):

$$\Pi = A_0\varphi^n \quad (6)$$

where $n \approx 2.31$ in a good solvent and $n = 3$ in Θ conditions. The numerical constant A_0 depends on the particular polymer–solvent pair.

In solutions the immediate vicinity of a given polymer segment is not uniform in concentration: due to repulsion of other polymer segments the region is locally depleted in polymer. The correlation length ξ appearing in eq 2 is the distance beyond which the solution returns to its average concentration. For dilute solutions, ξ is proportional to the size of the polymer coil. In the semidilute regime where different coils overlap, ξ defines the mean distance of approach between polymer segments. Π, which in scaling theory is proportional to kT/ξ^3, thus provides a measure of this distance in semidilute systems. From eq 6 it follows that in good solvent conditions

$$\xi \propto \varphi^{-0.77} \quad (7)$$

The principal difference between an un-cross-linked polymer and a network is that the latter cannot be diluted indefinitely by continued addition of solvent. Network swelling is limited by the opposing pressure of the elastic response that tends to shrink the network and expel the solvent.[13,16,17] In general the swelling pressure ω is

$$\omega = \Pi_g - G \quad (8)$$

where, Π_g is the osmotic contribution of the cross-linked polymer (mixing pressure) and G is the elastic modulus of the gel. In classical rubber elasticity theory,[16,17] G, the shear modulus, varies with polymer volume fraction φ as

$$G = G_0\varphi^m \quad (9)$$

G_0 is a constant that depends on the given network and $m = {}^1/_3$.

The compressional modulus for the gel, $K_{os} = \varphi(\partial\omega/\partial\varphi)$, is obtained from the concentration dependence of the swelling pressure ω.

Experimental Conditions

The PVAc gels were made from chemically cross-linked poly(vinyl alcohol) networks by acetylation, using a method described elsewhere.[18,19] Aqueous solutions of poly(vinyl alcohol) were cross-linked with glutaraldehyde at polymer concentration 6% w/w. Gel samples were prepared with two different molar ratios of monomer units to the molecules of the cross-linking agent, 50 and 200. The solutions were made in the concentration range $0.025 < \varphi < 0.13$ by dissolving a fractionated PVAc sample of molecular weight $M_n = 122\,000$ ($M_w/M_n < 1.1$) in acetone at 25 °C.

The X-ray scattering measurements were made on the D24 instrument on the DCI synchrotron at LURE Orsay. The incident white beam is focused by a curved monochromator through a Bragg angular deflection that selects the wavelength required for the experiment. The wavelength used here was 1.608 Å. The useful beam size is defined by a set of slits prior to the monochromator and two sets of antiscattering slits, one placed immediately after the monochromator and the other just before the sample. In the present experiments, the beam size was 3×0.5 mm^2.

The gels and solutions were contained in cells consisting of thin mica windows sealed in an air-tight stainless steel housing that prevented evaporation of the solvent. The spacing between the windows was defined by a 1-mm-thick stainless steel washer. The sample cells, which were lodged in a holder occupying 1.5 cm of air space in the X-ray beam, could be quickly replaced at the end of each run. A 6-cm linear gas-filled detector with a resolution of 256 points was situated 120 cm from the sample, and an evacuated tube with Kapton windows was placed in the intervening space. The beam stop, consisting of a 4-mm-wide tantalum rod of rectangular cross section, was positioned in the evacuated tube just in front of the detector.

The sample blanks for background subtraction consisted of pure acetone contained in the same cell as was used for the sample measurement; this procedure ensured that sample and background had identical thickness. Each run lasting 2×2000 s was preceded and followed immediately by a measurement of the sample transmission. This consisted of placing a thin sheet (ca. 1 mm) of amorphous carbon in the beam downstream of the sample for a preset time (50 s); the strong signal in the wings scattered from the carbon is proportional to the intensity of the incident beam transmitted by the sample, i.e., the product of the intensity incident on the sample I_0 and the sample transmission T. Excellent consistency was found between such transmission measurements and the independent primary beam monitor count from an ionization chamber. The corrected scattering signal from the sample thus becomes

$$I_{corr}(Q) = I_s(Q)/(I_{0s}T_st_s) - I_b(Q)/(I_{0b}T_bt_b)$$

where the subscripts s and b refer to the sample and background, respectively, and t is the corresponding counting time.

In principle, absolute scattering intensities of the samples can be calculated from the intensity scattered by density fluctuations of pure acetone, whose compressibility is known.[20,21] This signal, however, is weak and masked by scattering from the air in the gap housing the sample holder. In practice, the requisite calibration is achieved more readily by comparing the scattering signal of the polymer solutions with their measured osmotic pressure.

The swelling pressure was obtained by deswelling the swollen network surrounded by PVAc solutions of known toluene activity.[22] To prevent penetration by the polymer molecules the gels were enclosed in dialysis bags.[23]

The shear modulus of the gels G was determined at 25 °C as a function of the concentration, by uniaxial compression per-

Table I
Swelling Pressure and Elastic Parameters of PVAc–Acetone Gels at 25 °C

sample	φ	n	m	A/kPa	K_{os}/kPa[a]
6/50	0.106	2.24	0.328	4452	72.4
6/200	0.053	2.25	0.330	4386	14.7

[a] $K_{os} = A(n - m)\varphi^n$.

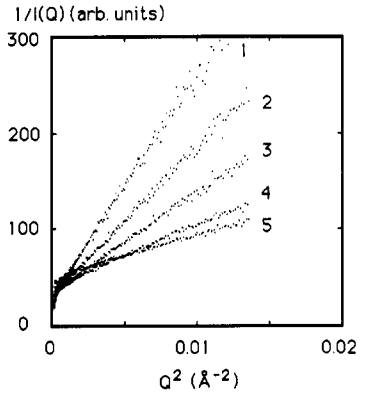

Figure 1. Zimm representation of corrected scattering spectra for the five PVAc–acetone solutions listed in Table II.

Table II
Characteristics of PVAc–Acetone Solutions and Gels Measured by SAXS

sample	φ	ξ/Å	$I(0)/10^3$	equiv vol fract	$10^3\langle\delta\varphi^2\rangle$
sol 1	0.0251	30.2	37.7		
sol 2	0.0426	22.3	32.4		
sol 3	0.0585	18.2	30.6		
sol 4	0.0880	14.3	26.2		
sol 5	0.1305	9.7	20.4		
gel 6/200	0.0530	35.9	43.5	0.023	0.25
gel 6/50	0.1060	13.4	26.2	0.088	8.3

formed at constant volume, in an apparatus described elsewhere.[24] The stress–strain data in the range of deformation ratio $0.7 \leq \Lambda < 1$ were evaluated by using the Mooney-Rivlin equation, which yielded C_2 equal to zero.

The mixing pressure Π_s was obtained by analyzing the swelling pressure data by using eq 8. The results are listed in Table I.

Results and Discussion

In Figure 1 the scattering spectra of PVAc–acetone solutions at five different concentrations are displayed in a Zimm representation. In the region $Q\xi \leq 1$, straight line behavior is observed for all concentrations. The correlation lengths ξ and intensities $I(0)$ resulting from the least-squares fits through the experimental points are listed in Table II. The concentration dependence of ξ is displayed in a double-logarithmic representation in Figure 2. The data through the four points of highest concentration obey a power law relation with an exponent close to that predicted by scaling theory (eq 7).

$$\xi = (2.2 \pm 0.2)\varphi^{-0.75\pm0.03}\ \text{Å} \qquad (10)$$

The point of lowest concentration in the figure, which lies slightly below the calculated straight line, has been omitted from the fit because its concentration is smaller than the overlap concentration[9] $\varphi^* \approx Pm/\rho R^3 = 6^{3/2}P^{-4/5}$ where m is the mass of the monomer unit, ρ is the density of the pure polymer, and R is the radius of gyration of the coil. In the present case P is approximately 1500, so that φ^* is in the vicinity of 0.04.

In polymer solutions the scattering intensity is given by eq 1, where the factor $a(\rho_p - \rho_s)^2$ is a constant for a given polymer–solvent system, and the only concentration-dependent quantity is φ^2/K_{os}. The compressional modulus K_{os} can be calculated from the variation of the osmotic pressure with concentration, the latter being available for the system PVAc–acetone in the literature.[22]

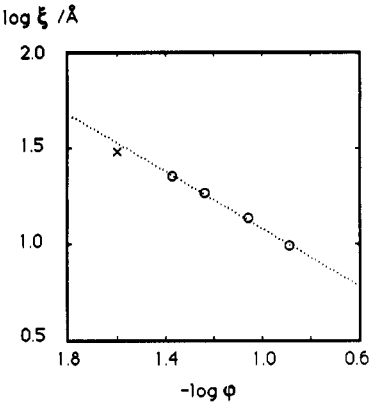

Figure 2. Double-logarithmic representation of the correlation length ξ as a function of polymer volume fraction φ. The straight line is a least squares fit through the four highest concentration points.

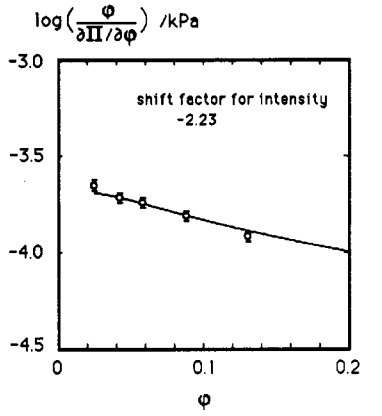

Figure 3. Values of $\varphi/(\partial\Pi/\partial\varphi)$ (kPa^{-1}) calculated from ref 20 (continuous line) on a logarithmic scale versus polymer volume fraction φ. Circles: observed SAXS intensity data for PVAc–acetone solutions, shifted down the vertical axis by a constant factor $0.00589 = 10^{-2.23}$.

Figure 3 shows the calculated dependence of φ^2/K_{os} versus φ (continuous curve) in a logarithmic representation. According to eq 1, measurement of $I(0)$ allows the constant proportionality factor $a(\rho_p - \rho_s)^2$ to be determined. This is done by shifting the intensities $I(0)$ (open circles) down the vertical logarithmic scale of this figure to give coincidence with the calculated curve. The best fit was found by applying a shift factor of −2.23 with respect to the arbitrary SAXS intensity scale. It can be seen that both $I(0)$ and φ^2/K_{os} display the same concentration dependence.

It can be concluded that the results from the solutions are consistent with scaling predictions and that the independent macroscopic osmotic pressure data provide an absolute calibration of the scattering intensity.

In Figure 4 the scattering spectrum of a fully swollen gel (6/200) is compared with that of a solution of almost the same concentration ($\varphi_{gel} = 0.053$, $\varphi_{sol} = 0.0585$). The qualitative difference between these two spectra is patent, the two curves crossing over in the region $Q \approx {}^1/_{30}$ Å^{-1}. At lower Q values the gel signal greatly exceeds that of the solution, while at higher Q values the opposite is true. This disparity demonstrates clearly that there is no simple correspondence between the solution-like behavior of the network polymer and that of the polymer solution at the same overall concentration. We are forced to conclude

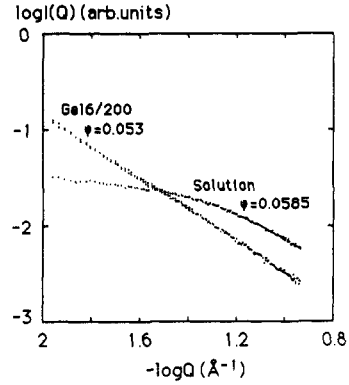

Figure 4. Comparison between scattering spectra of PVAc–acetone gel 6/200 ($\varphi = 0.053$) with that of solution at $\varphi = 0.0558$.

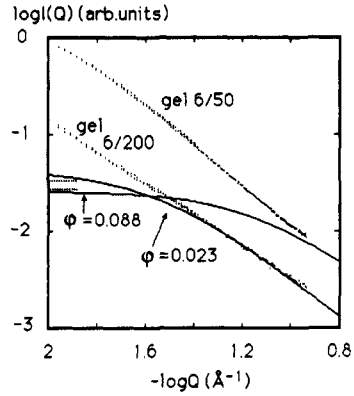

Figure 5. Spectra of gels 6/50 and 6/200 (experimental points). Continuous lines: spectra of solutions with φ adjusted so that the high-Q region of the spectra match the gels. The two dotted bars on the left vertical axis are the values of φ^2/K_{os} calculated from the swelling pressure data of each gel.

that the dynamic part of the spectrum resembles a solution at a different concentration. Inspection of Figure 4 suggests that in order to obtain agreement between the two spectra in the higher Q range, the effective correlation length (cf., eq 2) must be larger in the gel. This implies that the effective concentration of the solution that controls the scattering intensity of the network is lower than the average concentration.

Figure 5 shows how the solution-like part of the two gels investigated is estimated from their scattering signal. By varying φ, the values of $I_s(0)$ are calculated from eq 5, while ξ is calculated from eq 10. The continuous curves in Figure 5 are the resulting calculated solution spectra $I_s(Q)$ for concentrations $\varphi = 0.023$ and 0.088, respectively: only at these φ values was asymptotic coincidence between the solution and the gel scattering spectra found in the high Q region, i.e., where the static contribution to the gel signal becomes negligible. For both gels, these effective concentrations are considerably lower than the mean gel concentration. This result is consistent with the intuitive picture that the polymer concentration is enhanced around the cross-links points where movement is restricted and depleted elsewhere in the sample where the polymer segments are freer.

The extent of the permanent concentration deviations from uniformity is given by $\langle \delta\varphi^2 \rangle$. This quantity is calculated from Figure 5 by numerical integration of the difference in scattering intensities between the gel signal I_g and that of the effective corresponding solution I_s, using the relation

$$2\pi^2 V(\rho_p - \rho_s)^2 \langle \delta\varphi^2 \rangle = \int_0^\infty (I_g(Q) - I_s(Q)) Q^2 \, dQ \quad (11)$$

The values obtained for $\langle \delta\varphi^2 \rangle$ are shown in Table II. These results, which are close to those found by SANS for similar gels swollen in toluene, suggest that the static concentration fluctuations have a relative mean square amplitude $\langle \delta\varphi^2 \rangle / \langle \varphi \rangle^2$ of about 10% for sample 6/200 and 70% for sample 6/50. This shows that the extent of inhomogeneity strongly increases with cross-linking density. It has been shown previously[25] that such static fluctuations increase the intensity of the dynamically scattered light.

The independent swelling pressure data can be used to compare the forward scattering intensity of the solutions with the osmotic response of the gels. From the parameters listed in Table I the values of φ^2/K_{os}(gel), calculated for the two gel samples, are shown in Figure 5 as broken horizontal lines intersecting the vertical axis. Agreement with the estimated solution curves is striking.

These results seem to favor the presence of a solution-like component in the gel. For the PVAc–acetone gels investigated here, the scattering intensity of this component is effectively described by φ^2/K_{os}(gel).

Conclusions

The SAXS measurements reported here for semidilute PVAc–acetone solutions are in agreement with the predictions of scaling theory and display scattering behavior that is consistent with the osmotic properties of these solutions obtained from the literature. The osmotic data are used to normalize the SAXS spectra to yield absolute scattering intensities.

The gel scattering spectra are compared to those of the solutions, and the second moments describing the static concentration fluctuations are evaluated. For the two samples studied, these depend strongly on the cross-linking density. A solution-like component can be separated from the gel signal, the intensity of which is close to that calculated from independent osmotic measurements performed on the same samples. In both cases, the effective concentration of this component proves to be smaller than the mean concentration of the swollen network.

Acknowledgment. F.H. acknowledges the tenure of a Visiting Professorship at the Joseph Fourier University, Grenoble. This work is part of a joint CNRS–Hungarian Academy of Sciences project, both of which organizations are thanked for travel funds. We are also grateful to LURE for access to the D24 beam line.

References and Notes

(1) Hecht, A. M.; Duplessix, R.; Geissler, E. *Macromolecules* **1985**, *18*, 2167.
(2) Davidson, N. S.; Richards, R. W.; Maconnachie, A. *Macromolecules* **1986**, *19*, 434.
(3) Bastide, J.; Boué, F.; Buzier, M. In *Molecular Basis of Polymer Networks*; Baumgärtner, A., Picot, C. E., Eds.; Springer Proceedings in Physics 42; Springer: Berlin, 1989.
(4) Mallam, S.; Horkay, F.; Hecht, A. M.; Geissler, E. *Macromolecules* **1989**, *22*, 3356.
(5) Wu, W.; Shibayama, M.; Roy, S.; Kurokawa, H.; Coyne, L. D.; Nomura, S.; Stein, R. S. *Macromolecules* **1990**, *23*, 2245.
(6) Fang, L.; Brown, W. *Macromolecules* **1990**, *23*, 3284.
(7) Hamada, F.; Kinugasa, S.; Hayashi, H.; Hamada, F.; Nakajima, A. *Macromolecules* **1985**, *18*, 2290.
(8) Kinugasa, S.; Hayashi, H.; Hamada, F.; Nakajima, A. *Macromolecules* **1986**, *19*, 2832.
(9) de Gennes, P.-G. *Scaling Concepts in Polymer Physics*; Cornell: Ithaca, NY, 1979.
(10) Tanaka, T.; Hocker, L. O.; Benedek, G. B. *J. Chem. Phys.* **1973**, *59*, 5151.

(11) Mallam, S.; Horkay, F.; Hecht, A. M.; Rennie, A. R.; Geissler, E. *Macromolecules* **1991**, *24*, 543.
(12) Porod, G. *Small Angle X-ray Scattering*; Glatter, O., Kratky, O., Eds.; Academic Press: London, 1982.
(13) Flory, P. J. *Principles of Polymer Chemistry*; Cornell: Ithaca, NY, 1953.
(14) Muthukumar, M.; Edwards, S. F. *J. Chem. Phys.* **1982**, *76*, 2720.
(15) Muthukumar, M. *J. Chem. Phys.* **1986**, *85*, 4722.
(16) James, H. M.; Guth, E. J. *J. Chem. Phys.* **1943**, *11*, 455.
(17) Treloar, L. R. G. *The Physics of Rubber Elasticity*, 3rd ed.; Clarendon: Oxford, 1975.
(18) Horkay, F.; Nagy, M.; Zrinyi, M. *Acta Chim. Acad. Sci. Hung.* **1981**, *108*, 287.
(19) Horkay, F.; Zrinyi, M. *Macromolecules* **1982**, *15*, 1306.
(20) Bridgman, P. W. *The Physics of High pressure*; Dover: New York, 1970.
(21) Guinier, A.; Fournet, G. *Small angle Scattering of X-rays*; Wiley: New York, 1955.
(22) Vink, H. *Eur. Polym. J.* **1974**, *10*, 149.
(23) Nagy, M.; Horkay, F. *Acta Chim. Acad. Sci. Hung.* **1980**, *104*, 49.
(24) Horkay, F.; Nagy, M.; Zrinyi, M. *Acta Chim. Acad. Sci. Hung.* **1980**, *103*, 387.
(25) Geissler, E.; Hecht, A. M.; Horkay, F.; Zrinyi, M. *Macromolecules* **1988**, *21*, 2594.